Chemical Science

ARTICLE

Successive Light Induced Two Electron Transfers in a Ru-Fe Supramolecular Assembly : from Ru-Fe(II)-OH$_2$ to Ru-Fe(IV)-Oxo.

Christian Herrero,[a] Annamaria Quaranta,[b] Marie Sircoglou,[a] Katell Sénéchal-David,[a] Aurélie Baron,[b] Irene Mustieles Marín,[a] Charlotte Buron,[a] Jean-Pierre Baltaze,[a] Winfried Leibl,*[b] Ally Aukauloo,*[ab] and Frédéric Banse*[a]

In the present work we describe the synthesis and study of a Ru^{II}-Fe^{II} chromophore-catalyst assembly designed to perform the light-induced activation of an iron bound water molecule and subsequent photodriven oxidation of a substrate. Using a series of spectroscopic techniques, we demonstrate that excitation of the chromophore unit with 450 nm light, in the presence of a sacrificial electron acceptor, triggers a cascade of two electron transfers leading to the formation of a high-valent iron(IV)-oxo center from an iron(II) bound water molecule. The activity of this catalytic center is illustrated by the oxidation of triphenyl phosphine.

Introduction.

Despite the current efforts deployed to reduce the impact of human activities on the planet and reach sustainability, polluting and energy consuming chemical processes remain to be adjusted. This is particularly true for oxidation reactions where stoichiometric amounts of often toxic oxidants are commonly used.[1] In contrast, nature has developed several iron-based metalloenzymes that perform oxidation of organic substrates via high valent iron-oxo species.[2-4] To mimic these enzymes, a number of non heme polypyridyl complexes have been studied extensively and employed in different oxidation reactions including C-H bond cleavage, epoxidations, and sulfoxidations, using chemical oxidants such as PhIO, or peracids.[5,6] In these cases, the role of the oxidant used is twofold; it activates the Fe^{II} precursor by removal of two electrons to yield the active Fe^{IV}(O) intermediate, and acts as the source of oxygen atom that will ultimately be inserted in the reaction products. This "shunt" mechanism, which has been favored in this research field over the naturally occuring reductive activation of O$_2$ at iron centers, has proven to be an easier route to high valent iron-oxo centers but hinges on the use of the above mentioned oxygen containing oxidants.

An alternative methodology to performing such reactions involves the use of both visible light as source of energy, and water as a clean supply of electrons and O-atom in order to form energy rich reaction products. This approach, akin to the mechanism found in Photosystem II,[7,8] utilizes visible light in order to activate a chromophore, that in turn, triggers the successive oxidation of a catalytic center which activates a bound water molecule in the form of a metal-oxo species through a series of proton coupled electron transfer reactions (PCET) (Figure 1, Eqs 1-6).[9,10] This strategy has inspired the development of a new area of research whose goal is to develop synthetic models capable of transforming light energy into chemical energy stored in chemical bonds.[11-18]
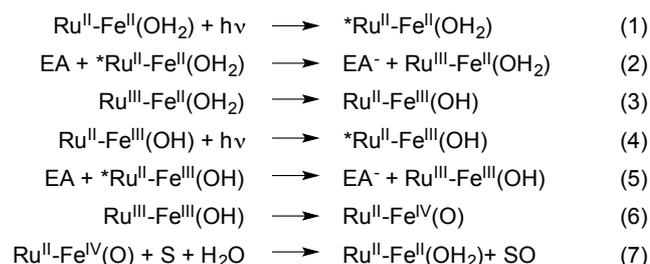
$$Ru^{II}\text{-}Fe^{II}(OH_2) + h\nu \longrightarrow {}^*Ru^{II}\text{-}Fe^{II}(OH_2) \quad (1)$$

$$EA + {}^*Ru^{II}\text{-}Fe^{II}(OH_2) \longrightarrow EA^- + Ru^{III}\text{-}Fe^{II}(OH_2) \quad (2)$$

$$Ru^{III}\text{-}Fe^{II}(OH_2) \longrightarrow Ru^{II}\text{-}Fe^{III}(OH) \quad (3)$$

$$Ru^{II}\text{-}Fe^{III}(OH) + h\nu \longrightarrow {}^*Ru^{II}\text{-}Fe^{III}(OH) \quad (4)$$

$$EA + {}^*Ru^{II}\text{-}Fe^{III}(OH) \longrightarrow EA^- + Ru^{III}\text{-}Fe^{III}(OH) \quad (5)$$

$$Ru^{III}\text{-}Fe^{III}(OH) \longrightarrow Ru^{II}\text{-}Fe^{IV}(O) \quad (6)$$

$$Ru^{II}\text{-}Fe^{IV}(O) + S + H_2O \longrightarrow Ru^{II}\text{-}Fe^{II}(OH_2) + SO \quad (7)$$

Figure 1. Overall mechanism to achieve oxygenation of a substrate by a Ru^{II}-Fe^{II} chromophore-catalyst complex upon light induced activation of a water molecule. EA and S denote electron acceptor and substrate molecules respectively. Protons released during steps 3 and 6 are omitted for clarity.

In our laboratories we have focused our efforts on the study of covalently bound chromophore-catalyst complexes designed to perform the visible-light activation of catalytic units.[19,20] Photo-activation of such assemblies triggers a series of energy

and electron transfer reactions which result in the formation of a charge-separated state where reductive equivalents are transferred onto a sacrificial electron acceptor while oxidative power is stored at the catalytic center.

In contrast to bimolecular chromophore/catalyst systems,[14,21] these assemblies are versatile tools that not only allow the study of the complete cascade of reactions that follow activation by visible light but offer the possibility to investigate the electronic communication between the chromophore and the catalyst. Furthermore, these types of assemblies are suitable candidates for their incorporation in dye sensitized photo-electrochemical cells, where as part of the photoanode,[22,23] they can furnish electrons and protons to a hydrogen, or fuel-forming cathode.

In this work, we report a full artificial photosynthetic system where light absorption, management of the chromophore's excited state, sequential electron transfer, accumulation of charges at the catalyst and catalysis are achieved and characterized. Using the chromophore-catalyst complex **1-OH$_2$** depicted in Figure 2, (for detailed synthetic procedure see Supporting Information), visible light as the sole source of energy and water as the O-atom source, we present the successive two-electron photo-oxidation of an iron-based catalyst. This process leads to the activation of a coordinated water molecule resulting in the formation of an active $Fe^{IV}(O)$ species that performs subsequent oxygen atom transfer onto a substrate (Figure 1). The two successive light induced oxidations of a metal-bound water have rarely been confirmed spectroscopically in the past.[24]
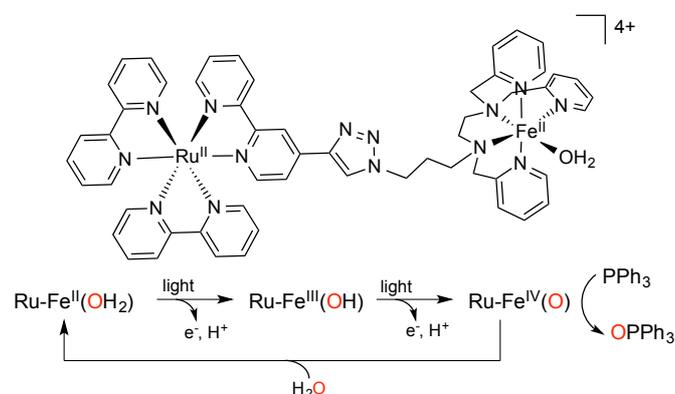

Figure 2. Structure of chromophore-catalyst complex **1-OH$_2$** used in this study, and simplified mechanism for the stepwise activation of the chromophore-catalyst complex prior to O-atom transfer.

Results and Discussion.

The chromophore employed is a $[Ru^{II}(bpy)_3]$-like complex whose excited state can be oxidatively quenched by a number of electron acceptors yielding a Ru^{III} state which has 1.30 V vs SCE of oxidative power (Figure 1. Eqs. 2, 5).[25] Depending on the experiments performed, the electron acceptors used were either methyl viologen or $[Co^{III}(NH_3)_5Cl]^{2+}$ salts which, unlike

4-nitrobenzene diazonium and sodium peroxosulfate that were also tried, were the only acceptors able to oxidatively quench the excited state of the ruthenium chromophore without performing the oxidation of the Fe^{II} catalyst unit in the absence of light.[26] The catalyst is an Fe^{II} ion wrapped by a pentadentate amine/pyridine ligand (noted L_5^2 hereafter), known to perform the catalytic oxidation of organic substrates in presence of oxygen containing oxidants and for which the spectroscopic signature of the $Fe^{IV}(O)$ intermediate has been reported.[27-29]

The Ru^{II}-Fe^{II} complex was first isolated with a chloro exogenous ligand bound to Fe^{II} (**1-Cl**, see Supporting Information). When dissolved in 4:1 $H_2O:CH_3CN$ (WAN), this complex exhibits two strong absorptions at 450 nm ($\varepsilon = 17000$ $M^{-1}cm^{-1}$) due to a Ru^{II} to ligand charge transfer band (MLCT) and at 280 nm arising from bipyridine π-π* transitions (Figure SI 6). Additionally, the absorption spectrum exhibits a shoulder at 400 nm ($\varepsilon = 5000$ $M^{-1}cm^{-1}$) which coincides with the absorption maximum observed for the $[(L_5^2)Fe^{II}(OH_2)]^{2+}$ reference compound **2-OH$_2$** (Figures SI 5 and SI 6) arising from a Fe^{II} to π*pyridine charge transfer band. In a 4:1 WAN mixture the chloro ligand is thus substituted by water leading to the Ru-$Fe^{II}(OH_2)$ precursor (**1-OH$_2$**).[30,31]

This ligand substitution was further confirmed by electrochemical studies. For the synthetically prepared reference compound **2-OH$_2$** the $Fe^{III}(OH_2)/Fe^{II}(OH_2)$ redox signal is observed at 0.51 V vs. SCE ($\Delta E = 140$ mV) in acetone. This value matches the one obtained for **2-Cl** when studied in a 4:1 WAN solvent mixture ($E_{1/2} = 0.46$ V) (Figure SI 7). Complexes **1-Cl**, **1-CH$_3$CN**, and **1-OH$_2$** were also prepared and studied by cyclic voltammetry (CV). In each case two different reversible processes are observed at positive potentials. A first, ligand-independent process corresponding to the Ru^{III}/Ru^{II} couple is observed at $E_{1/2} = 1.26$ V vs. SCE ($\Delta E = 68$ mV). A second wave, the potential of which varies as a function of the exogenous ligand bound to Fe, is attributed to the $Fe^{III/II}$ couple and is observed at either 0.97 V, 0.60 V or 0.50 V vs. SCE for **1-CH$_3$CN**, **1-Cl** or **1-OH$_2$** respectively (Figure SI 8). In any case, our electrochemical data for complexes **1** indicate that (i) the Fe^{III}-X/Fe^{II}-X potential is almost identical to the one of model complex **2-X** (X = CH_3CN, Cl or H_2O); and (ii) a photogenerated Ru^{III} center should have enough driving force to oxidize the covalently linked $[(L_5^2)Fe^{II}]$ unit regardless of the nature of the exogenous ligand (Table S1).

The excited state properties of the photosensitizer (*Ru^{II}) in **1** were studied using steady state and time-resolved fluorescence spectroscopy techniques. Emission of **1-OH$_2$** in 4:1 WAN is strongly quenched compared to the reference compound $[Ru(bpy)_3]^{2+}$ ($\lambda_{max} = 605$ nm, $\Phi = 0.059$)[25] and shows a maximum at 619 nm with a quantum yield of 0.0091. Emission decay, as often observed for dinuclear complexes based on $[Ru(bpy)_3]^{2+}$ chromophores,[32,33] is biphasic with a main component of ~80 ns (65%) and a minor one of ~600 ns (35%). The excited state quenching is tentatively assigned to an energy transfer mechanism between the chromophore's excited state and low lying metal centered states of the catalyst unit since an electron transfer mechanism from the catalyst to the

excited state of the chromophore can be ruled out by ligand exchange experiments (Table SI 1 and accompanying text) and a resonance energy transfer process is not consistent with the absorption/emission properties of the donor (Ru) and acceptor (Fe). Furthermore, the spin state of the Fe^{II} complex was found not to influence this quenching as the same phenomenon was observed in the case of the low spin (S=0) cyano derivative $[(L_5^2)Fe^{II}(CN)]^+$.
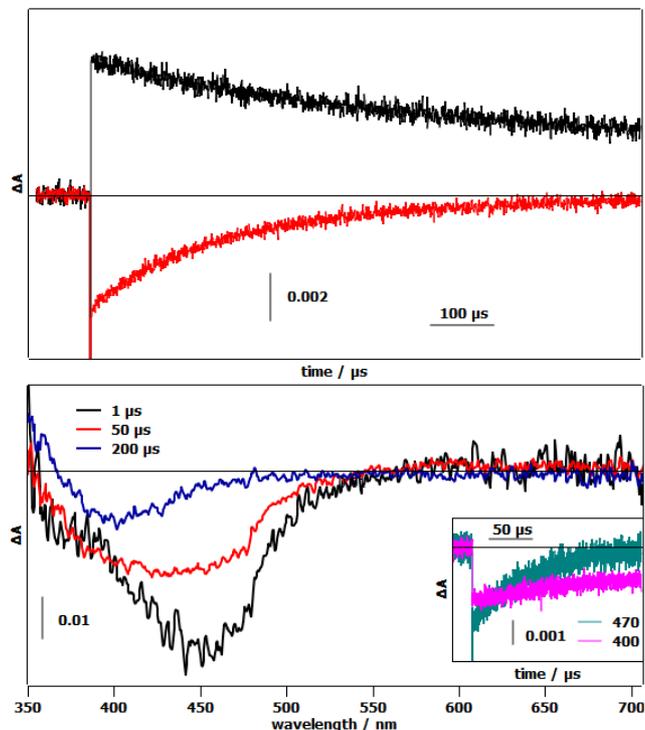

Figure 3. Top) transient absorption kinetics of **1-OH$_2$** in presence of 20 mM methylviologen (MV^{2+}) after 460 nm laser flash excitation. Black trace : decay of $MV^{\bullet+}$ to MV^{2+} followed at 605 nm. Red trace: recovery of Ru^{II} from Ru^{III} monitored at 450 nm. Bottom) Transient absorption spectra of **1-OH$_2$** in presence of 20 mM $[Ru^{III}(NH_3)_6]Cl_3$ at 1, 50, and 200 μs after laser flash excitation. Inset: kinetic traces for the recovery of Ru^{II} (470 nm, green trace) and the disappearance of Fe^{II} (400 nm, pink trace). Laser energy: 10 mJ.

The first photoinduced electron transfer (Figure 1, Eq. 3) was studied by laser flash photolysis. The differential absorption traces after excitation of **1-OH$_2$** in presence of methyl viologen (MV^{2+}) as reversible electron acceptor in a 4:1 WAN mixture, showed an increase of absorption at 605 nm together with a bleach at 450 nm (Figure 3, top). These absorption changes are probes of the reduction of methyl viologen ($MV^{2+} \rightarrow MV^{\bullet+}$) and the concomitant formation of the oxidized state of the chromophore ($Ru^{II} \rightarrow Ru^{III}$) (Figure 1, Eq. 1-2). Recovery of the chromophore's ground state is approximately 5 times faster than that of MV^{2+} implying an intramolecular electron transfer between the reduced form of the catalytic module and the oxidized chromophore (Ru^{III}-Fe^{II} $\rightarrow$ Ru^{II}-Fe^{III}) (Figure 1, Eq. 3). To investigate the changes in

electronic absorption features occurring during the electron transfer process we replaced MV^{2+} by $[Ru^{III}(NH_3)_6]Cl_3$, which does not absorb in the visible region (Figure 3, bottom). The strong initial bleaching of the Ru^{II} MLCT at 450 nm after excitation evolves in ~60 μs into a depletion band with a maximum at 400 nm (Figure 3, bottom) that is attributed to the formation of the Fe^{III} state in the catalytic module. This loss of absorption at 400 nm, which originates from the loss of the Fe^{II} to $\pi^*_{pyridine}$ MLCT band, was also observed upon chemical oxidation of **1-OH$_2$**, and more so with reference compound **2-OH$_2$**, when they were treated with 2 equivalents of H_2O_2 (Figure SI 9).

To further study the change in oxidation state of the initial Fe^{II} ion, we performed X-band EPR measurements after continuous light excitation of a solution of **1-OH$_2$** in 4:1 WAN in presence of $[Co^{III}(NH_3)_5Cl]^{2+}$ acting as an irreversible electron acceptor. The initial spectrum shows no observable signal due to the diamagnetic nature of the Co^{III} and Ru^{II} ions and the high spin Fe^{II} S = 2 state (Figure 4, left, blue trace). After irradiation of this sample with 450 nm light for 2 min, the EPR spectrum exhibits a resonance at g = 4.44 due to formation of high spin Co^{II} ions in solution and signals at g = 2.34, 2.15, 1.91 which are characteristic of low spin $Fe^{III}(OH)$ (S = ½) in this family of complexes (Figure 4, left, red trace).[21,34-36] Furthermore, these resonances match those observed when **1-OH$_2$** is chemically oxidized using 2 eq. H_2O_2 (Figure 4, right). In parallel, results of a controlled chemical oxidation performed on reference compound **2-OH$_2$** are consistent with the above observation (Figure SI 10). Altogether these results clearly evidence the first activation step of the Fe-bound water molecule leading to Ru^{II}-$Fe^{III}(OH)$.
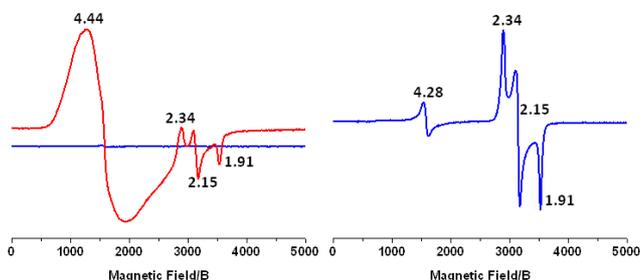

Figure 4. X-band EPR of: Left) 16 mM $[Co^{III}(NH_3)_5Cl]^{2+}$ and 0.80 mM complex **1-OH$_2$** in a 4:1 H_2O:CH_3CN solvent mixture before (blue) and after (red) 2 min 450 nm illumination time. Right) 1.65 mM solution complex **1-OH$_2$** after addition of 2 eq. H_2O_2. The weak resonance at g 4.28 is due to ubiquitous S=5/2 Fe^{III} species.

The second light-induced electron transfer (Figure 1, Eq. 6) needed to generate the targeted $Fe^{IV}(O)$ species was evidenced by studying the evolution of the EPR signal at different time intervals during continuous illumination of a solution of **1-OH$_2$** in 4:1 WAN in presence of $[Co^{III}(NH_3)_5Cl]^{2+}$. An increase in intensity of the EPR signals accounting for the formation of the low spin $Fe^{III}(OH)$ species was observed, followed by its decrease until complete disappearance of the rhombic low-spin

Fe^{III} signal (Figure SI 11). Concomitantly, we observed a persistent increase of the signal related to the photo-reduced free Co^{II} ions in solution. These observations are supportive of a second electron transfer process from the Fe^{III}(OH) intermediate to photogenerated Ru^{III} leading to the probable formation of a low spin S=1 Fe^{IV} species. A conclusive kinetic study of this second electron transfer by laser flash photolysis of Ru^{II}-Fe^{III}(OH) (prepared with H$_2$O$_2$) in presence of MV^{2+} has not yet been possible due to competitive back electron transfer processes between the reduced reversible electron acceptor and the singly oxidized Fe^{III}(OH) form of the catalyst (Figure SI 12). Definitive evidence for the photogeneration of an Fe^{IV}(O) species comes from the ESI-MS characterization of an irradiated solution of **1-OH$_2$** under similar experimental conditions. The mass spectrum shows a signal at 688.1087 amu corresponding to {[Ru^{II}-Fe^{IV}(O)](PF$_6$)(OTf)}$^{2+}$ (Figure 5, top). Isotopic labelling experiments with H$_2$^{18}O were performed to confirm the origin of the oxygen atom in the metal oxo species. A peak at 689.1026 was detected corresponding to {[Ru^{II}-Fe^{IV}(^{18}O)](PF$_6$)(OTf)}$^{2+}$. This result evidences that the oxidized form Fe^{IV}(O) stems from the activation a metal-bound water molecule. Additionally, the formation of the Fe^{IV}(O) species was revealed by its characteristic absorbance band at 750 nm (Figure SI 13) which compares well with the reported values 756 nm for [(L$_5$^{2})Fe^{IV}(O)]$^{2+}$.[29]
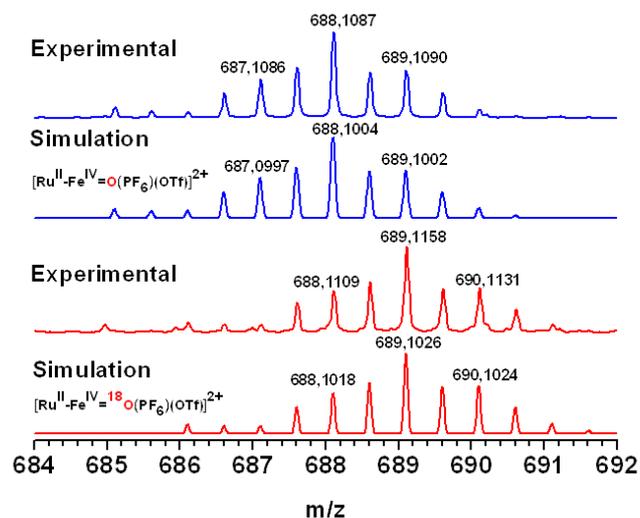

Figure 5. HR ESI-MS of Ru^{II}-Fe^{IV}(O) produced after illumination of complex **1-OH$_2$** with 450 nm light in presence of H$_2$O (blue) or H$_2$^{18}O (red). Simulation spectra are shown for comparison of isotopic patterns.

A preliminary investigation of the catalytic activity of the photogenerated Fe^{IV}(O) species was performed using triphenyl phosphine as the substrate. Reaction mixtures containing complex **1-OH$_2$**, [Co^{III}(NH$_3$)$_5$Cl]$^{2+}$, triphenyl phosphine and acetate buffer in 4:1 WAN mixture were illuminated with 450 nm light. GC monitoring showed the formation of increasing amounts of triphenyl phosphine oxide during the first 10 minutes of illumination (Figure SI 14) reaching a turnover number (TON) of 3.2. This TON corresponds to a 20% efficiency with respect to the amount of [Co^{III}(NH$_3$)$_5$Cl]$^{2+}$ used, which in our case, is the limiting reagent. Removal of any of the components in the reaction mixture, [Co^{III}(NH$_3$)$_5$Cl]$^{2+}$, complex **1-OH$_2$**, substrate, light, as well as substitution of complex **1-OH$_2$** by [Ru(bpy)$_3$]$^{2+}$ yielded no oxidation product during control runs. Proof of the insertion of oxygen from water in the substrate was obtained by use of H$_2$^{18}O and the detection of isotopically labelled triphenylphosphine oxide (Figure SI 15).

Conclusion.

In summary, we have put in evidence the two sequential light-induced electron transfer reactions from a Fe^{II}(OH$_2$) species to a covalently bound chromophore and subsequent oxygen atom transfer from the resulting Fe^{IV}(O) intermediate. After the first photon absorption, the one-electron oxidized intermediate Ru^{II}-Fe^{III}(OH) has been identified by X-band EPR and flash photolysis methods. Further illumination of this species leads to the Ru^{II}-Fe^{IV}(O) intermediate which has been characterized by ESI-MS and UV-visible. Oxygen –atom transfer from the Fe^{IV}(O) moiety to triphenylphosphine has been proven using ^{18}O labelling experiments.

While the present work confirms the validity of the concept, current efforts in our laboratories are directed towards the optimization of the system. These include the improvement of the excited state properties of the chromophore-catalyst assembly in order to optimize the photo-driven electron transfer processes, the implementation of a more potent oxidation catalyst, as well as synthetic modification for its incorporation in Graetzel-type semiconducting electrodes[23] in order to both avoid the use of sacrificial electron acceptors, and to recover the electrons obtained during light-driven oxidation reactions for their further use.

Acknowledgments

Notes and references

1.   J. A. Labinger, *J. Mol. Catal. A*, 2004, **220**, 27–35.

2.　P. C. A. Bruijnincx, G. van Koten, and R. J. M. Klein Gebbink, *Chem. Soc. Rev.*, 2008, **37**, 2716.

3.　M. Costas, M. P. Mehn, M. P. Jensen, and L. Que, *Chem. Rev.*, 2004, **104**, 939–986.

4.　C. Krebs, D. Galonić Fujimori, C. T. Walsh, and J. M. Bollinger, *Acc. Chem. Res.*, 2007, **40**, 484–492.

5.　W. Nam, *Acc. Chem. Res.*, 2007, **40**, 522–531.

6.　W. Nam, Y.-M. Lee, and S. Fukuzumi, *Acc. Chem. Res.*, 2014, **47**, 1146–1154.

7.　J. Barber, *Chem. Soc. Rev.*, 2009, **38**, 185.

8.　J. P. McEvoy and G. W. Brudvig, *Chem. Rev.*, 2006, **106**, 4455–4483.

9.　T. J. Meyer, M. H. V. Huynh, and H. H. Thorp, *Angew. Chem. Int. Ed.*, 2007, **46**, 5284–5304.

10.　M. H. V. Huynh and T. J. Meyer, *Chem. Rev.*, 2007, **107**, 5004–5064.

11.　M. E. Ener, Y.-T. Lee, J. R. Winkler, H. B. Gray, and L. Cheruzel, *Proc. Natl Acad. Sci. USA*, 2010, **107**, 18783–18786.

12.　S. Fukuzumi, T. kishi, H. Kotani, Y. M. Lee, and W. Nam, *Nature Chem*, 2011, **3**, 38–41.

13.　G. Knör, *Chem. Eur. J.*, 2009, **15**, 568–578.

14.　H. Kotani, T. Suenobu, Y.-M. Lee, W. Nam, and S. Fukuzumi, *J. Am. Chem. Soc.*, 2011, **133**, 3249–3251.

15.　O. Hamelin, P. Guillo, F. Loiseau, M.-F. Boissonnet, and S. Ménage, *Inorg. Chem.*, 2011, **50**, 7952–7954.

16.　H. Inoue, T. Shimada, Y. Kou, Y. Nabetani, D. Masui, S. Takagi, and H. Tachibana, *ChemSusChem*, 2011, **4**, 173–179.

17.　D. W. Low, J. R. Winkler, and H. B. Gray, *J. Am. Chem. Soc.*, 1996, **118**, 117–120.

18.　F. Li, Y. Jiang, B. Zhang, F. Huang, Y. Gao, and L. Sun, *Angew. Chem. Int. Ed.*, 2012, **51**, 2417–2420.

19.　C. Herrero, A. Quaranta, R.-A. Fallahpour, W. Leibl, and A. Aukauloo, *J. Phys. Chem. C*, 2013, **117**, 9605–9612.

20.　C. Herrero, A. Quaranta, W. Leibl, A. W. Rutherford, and A. Aukauloo, *Energy Environ. Sci.*, 2011, **4**, 2353–2365.

21.　A. Company, G. Sabenya, M. González-Béjar, L. Gómez, M. Clémancey, G. Blondin, A. J. Jasniewski, M. Puri, W. R. Browne, J.-M. Latour, L. Que Jr., M. Costas, J. Pérez-Prieto, and J. Lloret-Fillol, *J. Am. Chem. Soc.*, 2014, **136**, 4624–4633.

22.　A. Nayak, R. R. Knauf, K. Hanson, L. Alibabaei, J. J. Concepcion, D. L. Ashford, J. L. Dempsey, and T. J. Meyer, *Chem. Sci.*, 2014, **5**, 3115–3119.

23.　D. L. Ashford, W. Song, J. J. Concepcion, C. R. K. Glasson, M. K. Brennaman, M. R. Norris, Z. Fang, J. L. Templeton, and T. J. Meyer, *J. Am. Chem. Soc.*, 2012, **134**, 19189–19198.

24.　J. Berglund, T. Pascher, J. R. Winkler, and H. B. Gray, *J. Am. Chem. Soc.*, 1997, **119**, 2464–2469.

25.　A. Juris, V. Balzani, F. Barigelleti, S. Campagna, P. Belser, and A. Von Zelewsky, *Coord. Chem. Rev.*, 1988, **84**, 85–277.

26.　A. R. Parent, R. H. Crabtree, and G. W. Brudvig, *Chem. Soc. Rev.*, 2013, **42**, 2247.

27.　N. Ségaud, J.-N. Rebilly, K. Sénéchal-David, R. Guillot, L. Billon, J.-P. Baltaze, J. Farjon, O. Reinaud, and F. Banse, *Inorg. Chem.*, 2013, **52**, 691–700.

28.　A. Thibon, J.-F. Bartoli, S. Bourcier, and F. Banse, *Dalton Trans.*, 2009, 9587.

29.　V. Balland, M.-F. Charlot, F. Banse, J.-J. Girerd, T. A. Mattioli, E. Bill, J.-F. Bartoli, P. Battioni, and D. Mansuy, *Eur. J. Inorg. Chem.*, 2004, **2004**, 301–308.

30.　P. Comba, H. Wadepohl, and A. Waleska, *Aust. J. Chem.*, 2014, **67**, 398–404.

31.　A. Draksharapu, Q. Li, H. Logtenberg, T. A. van den Berg, A. Meetsma, J. S. Killeen, B. L. Feringa, R. Hage, G. Roelfes, and W. R. Browne, *Inorg. Chem.*, 2012, **51**, 900–913.

32.　M. L. A. Abrahamsson, H. B. Baudin, A. Tran, C. Philouze, K. E. Berg, M. K. Raymond-Johansson, L. Sun, B. Åkermark, S. Styring, and L. Hammarström, *Inorg. Chem.*, 2002, **41**, 1534–1544.

33.　C. Herrero, L. Batchelor, A. Baron, S. El Ghachtouli, S. Sheth, R. Guillot, B. Vauzeilles, M. Sircoglou, T. Mallah, W. Leibl, and A. Aukauloo, *Eur. J. Inorg. Chem.*, 2013, 494–499.

34.　M. Martinho, P. Dorlet, E. Rivière, A. Thibon, C. Ribal, F. Banse, and J.-J. Girerd, *Chem. Eur. J.*, 2008, **14**, 3182–3188.

35.　G. Roelfes, M. Lubben, K. Chen, R. Y. N. Ho, A. Meetsma, S. Genseberger, R. M. Hermant, R. Hage, S. K. Mandal, V. G. Young, Y. Zang, H. Kooijman, A. L. Spek, L. Que, and B. L. Feringa, *Inorg. Chem.*, 1999, **38**, 1929–1936.

36.　L. Duelund, R. Hazell, C. J. McKenzie, L. Preuss Nielsen, and H. Toftlund, *J. Chem. Soc., Dalton Trans.*, 2001, 152–156.